Acoustic Impedance (AI) Inversion for Porosity and Reservoir Quality Prediction in Kakawa Field, Onshore Niger Delta

Magnus O. Kanu, I. Tamunobereton-ari, O. I. Horsfall

Abstract: In this study, the transforming of seismic reflection data into an intrinsic rock property model in Kakawa field, onshore Niger delta, Nigeria have been quantitatively examined. Specifically, an application of a methodology that allows interpreters to obtain porosity distribution from post-stack 3D seismic amplitude data, using measured density and sonic well log data as constraints, is presented here. 3D acoustic impedance model was calculated from seismic reflection amplitudes by applying a constrained sparse-spike inversion algorithm. Also, a 3D low-frequency impedance model was estimated by kriging of impedance values calculated from well log data and added to the inversion result to provide a full band or absolute acoustic impedance model. The major component of this study was establishing the relationship between the P-impedance and porosity using well-log data and this was used to convert the full band acoustic impedance model into a porosity volume. This was key input into static and dynamic modelling which supported the formulation of a field development plan (FDP) for the Kakawa field. The results from the study showed that there is a good agreement between the modelled impedance and the in-situ log-derived impedance across the E1000 reservoir, also the detailed acoustic impedance volume was key in assessing lateral variability and extent of reservoir and aided validation of seismic interpretation. These results can be applied successfully to aid reservoir characterization in Niger delta, Nigeria.

Key words: *Acoustic Impedance, Reservoir, Rock Physics, Seismic Inversion*

INTRODUCTION

The presence of a porous reservoir rock with appropriate geological structure, an effective seal and a mature source rock are some of the elements of an effective petroleum system. While there are a number of geophysical methods of finding petroleum systems, seismic method is the most important as it enables determining the volumes of hydrocarbons in a reservoir for field development decisions.

Many studies have shown that porosity is the most important factor in determining the seismic response (Rafavich et al., 1984; Wang et al., 1991; Anselmetti and Eberli, 1993). Inversion of seismic data is a well-known oil- and gas-industry tool used for refining structural interpretation and reservoir characterization (reservoir geometry, property prediction). It is the process of determining what physical characteristics of rocks and fluids (i.e., P-impedance, S-impedance, and density) could have produced the observed seismic data.

Three-Dimensional (3D) Porosity estimation from a Seismically-Constrained Reservoir modeling involves inferring elastic rock property (density and velocity) inter-well from three-dimensional seismic data through a process of solving the "inverse problem" and using well-calibrated transformations of these properties to predict reservoir porosity.

Seismic inversion is an integration tool for the construction of seismic-scale reservoir models that are consistent with rock physics knowledge, well data, and seismic amplitude information. Asset teams can reduce exploration and development risk by working from a common subsurface description or characterization that is the product of integrating the data of the various geoscience disciplines. In order to work effectively, this subsurface description must be a common data type that is understood by all geoscientists. Acoustic Impedance (AI) is this common data type. AI is an ideal medium for integrating well logs and the seismic data since the impedance values from the inversion can be directly related to layer-based rock properties. Reservoir properties can be derived from impedance for reservoir modelling.

According to Tarantola, A. (2005), rock physics analysis is the key to relating the seismic properties to reservoir properties and high-quality seismic reservoir characterization requires well log data that are consistent between formations and wells over the entire vertical interval of interest and represent the true undisturbed rock properties.

GEOLOGIC SETTING

The Kakawa field is located approximately 100 km NW of Port Harcourt. It is among the fields identified as partially appraised fields (PAF) or unappraised discoveries as opportunities for non-associated gas development. The field was discovered in 1977 by exploration well K-01 and up to date, only two additional wells have been drilled.

- *Magnus Kanu: Department of Physics, Faculty of Science, Rivers State University, Port Harcourt Nigeria (Corresponding Author)*
- *Dr I. Tamunobereton-ari: Department of Physics, Faculty of Science, Rivers State University, Port Harcourt Nigeria*
- *Dr O. I. Horsfall: Department of Physics, Faculty of Science, Rivers State University, Port Harcourt Nigeria*

The Field is an Early Miocene to Late Oligocene channel sands and comprises a series of interlocking gentle elongate NW-SE trending rollover anticlines. The structure of the field is large, bounded by boundary faults to the North and to the South. A total of twelve (10) stacked reservoirs have been penetrated between 7500 and 11250 ftss and the main hydrocarbon-bearing reservoirs in the field are the E1000, F1000 and D7000. The reservoirs consist predominantly of shoreface deposits that were later cut by channels, all deposited in wave-dominated, high-energy deltaic setting.

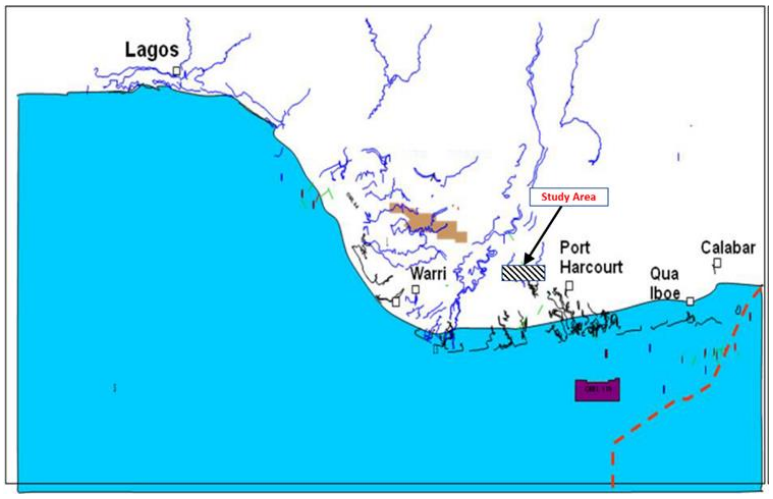

Figure 1: Map of the Niger Delta showing the study area (Kakawa field).

DATA AVAILABILITY AND QUALITY

The field is covered by 3D seismic data, acquired in 1998. The shot and receiver line spacing were 500m and 350m respectively, while shot and receiver points were spaced 50m apart. The data was processed and re-processed in many times, the latest processing being a Kirchhoff Pre-Stack Depth Migrated (PSDM) volume which was done in 2017 and was used for this study. The quality of the seismic data is generally good especially down to 3.5 seconds TWT (two-way-time), characterized by prominent seismic events that show good lateral continuity. The data has been processed as a zero-phase wavelet with a negative polarity displayed as a trough that characterizes an increase in acoustic impedance. Frequency spectrum of seismic data shows that frequency content is between 7Hz and 47Hz. Beyond 47Hz, noise dominates signals. Below 7Hz presents the frequency gap in the seismic data. Amplitude analysis indicates seismic data has balanced amplitude as shown in the symmetric amplitude distribution

A total of 3 wells, K-01, K-02 and K-10. have been drilled to date in the field. A suite of logs consisting of compressional sonic, density, GR, resistivity, porosity and calliper exists for all wells. They are however, of varying degrees of quality requiring petrophysical log editing and data conditioning before use. Well-bore acquired check-shots (TZ) information is only available in K-01 and K-10, forming the basis for the well-to-seismic ties and wavelet extraction. K-01 check-shot was used for similar exercise in K-02. The horizon interpretation for E1000 looks good and covers the area of interest. There is also reservoir top and base for the objective sand E1000.

METHODOLOGY

Rock Physics Analysis

Rock physics analysis provides the link between rock properties and seismically derived elastic properties and is very useful for the meaningful assessment of a geologic model and any quantitative integration of seismic, well, and core data. The objective of rock physics analysis is to determine the measured data that best discriminate lithologies across the reservoirs of interest. A lithology discrimination diagnostic cross plot was made to understand if it is possible to separate sands from shale. This feasibility study therefore underpins the prediction of reservoir sands from seismically derived P-impedance away from well penetration

From analysis as seen in Figure 2, we deduce that reservoir sands are acoustically softer than adjacent shales. The gamma ray log has strong linear relationship with acoustic impedance, clearly discriminating sands and shales. This wire line cross plot establishes framework within which inverse model derived impedance can be interpreted.

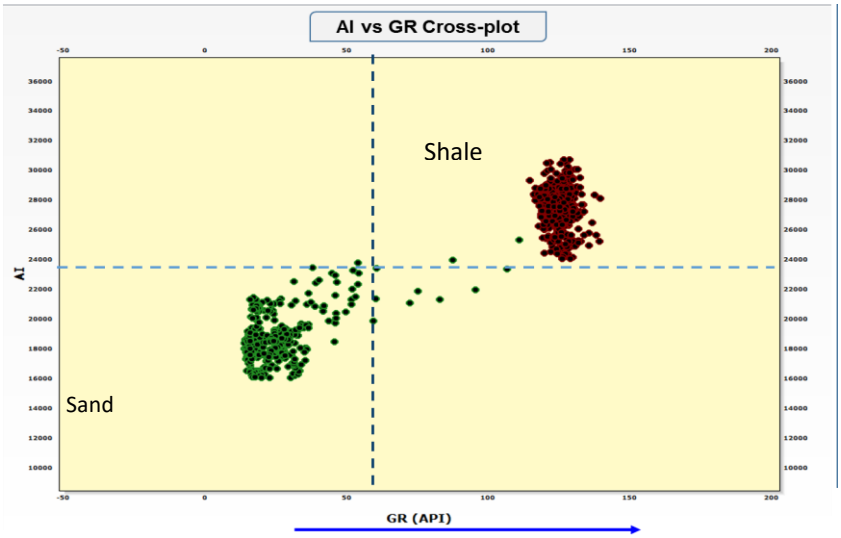

Figure 2: Wire-line log crossplot of gamma-ray values vs. acoustic impedance graded by gamma ray. The gamma-ray values have strong linear relationships with acoustic impedance.

Seismic Inversion

An important aspect of the inversion workflow is the estimation of seismic wavelet. The aim of wavelet estimation [either from single or multiple wells] is to find a wavelet which when used to invert the seismic data at the well locations will yield acoustic impedance that match the well log acoustic impedance. This is with the proviso that all data are reliable after match compensation has been carried out for differences in scale and frequency content of the different surveys [seismic and well logging]. This was carried out deterministically through robust well-to-seismic ties for the three wells. Wavelet analysis was conducted by computing a filter that best shaped the well log reflection coefficients to the input seismic data at the three well locations. Some differences were observed in the wavelets in terms of the side-lobes, amplitude and phase. Due to these variabilities, it was decided to calculate an average wavelet for use in the seismic inversion process. The average wavelet was characterized by an envelope centred around zero, tails taper off to zero and low order side lobes. It has a smooth amplitude spectrum without notches and flat near zero phase spectrum within the seismic bandwidth. The estimated wavelets at the respective wells and the average wavelet are shown below.

A model wavelet was estimated (Figure 3B) to match the amplitude, phase and frequency of the processed seismic data and convolved with the reflectivity coefficient series from the log P-impedance. This process yields a synthetic seismic trace that compares nicely with the input seismic trace with correlation coefficient of 80% indicating minor residual between seismic and synthetics (Figure 3A).

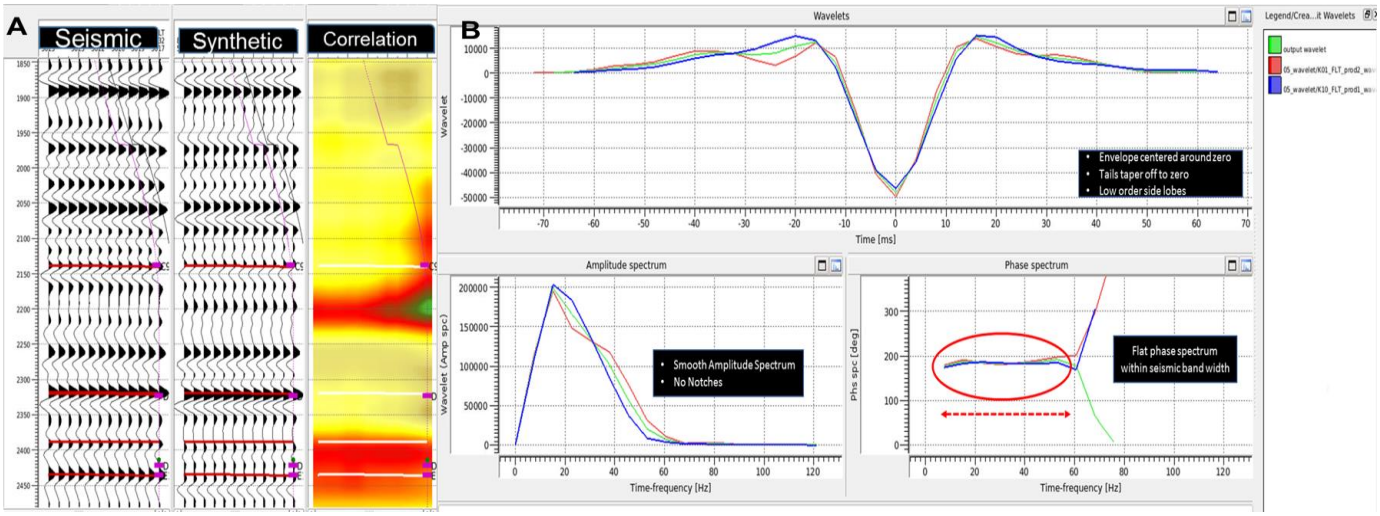

Figure 3: A) Well to seismic tie and correlation panel for K-10 well showing great match between seismic traces and the adjacent synthetic seismogram displayed in wiggle trace. B) derived average wavelet (green colour) computed from the best wavelets

After wavelet estimation, it was to compensate for the gap in seismic frequency spectrum. It was determined during the feasibility study that the seismic data lacked 0-7 Hz frequencies. See Figure 4. For this, a Low Frequency Model (LFM) was built and supplied to the inversion workflow. An Earth model framework was created to represent the structural geometry of the field. A solid model was then created by interpolating and extrapolating impedance from the wells, guided by the Earth model framework. The Earth model provided the low frequency end of the final model. The low frequencies are most critical to rock properties because it leads to determining fluid, porosity and other reservoir properties needed to make drilling decision.

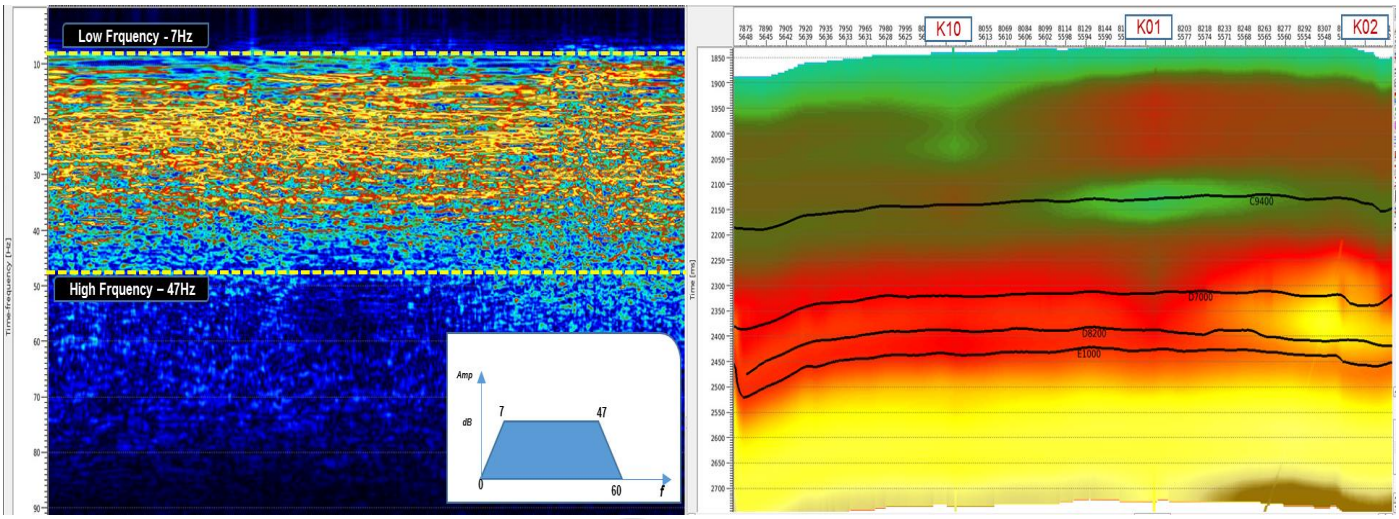

Figure 4: Left: Frequency spectrum showing seismic data has a frequency gap of 0 – 7 Hz. Right: Traverse of Low frequency (0-7 Hz) model through key wells showing very good match at the wells both qualitatively and quantitatively

The 3D seismic data was inverted using Jason Geoscience Workbench (JGW) Constrained Sparse Spike Inversion algorithm (CSSI). The CSSI models input seismic data by convolving the estimated wavelet and a sparse reflection coefficient series representing the geology. Constraints were imposed in order to find the best geological and geophysical solution. These constraints provided by geophysical bounds, described how the impedance could vary laterally away from the wells. In addition, the well log impedance defines low frequency trends. Optimum Acoustic Impedance (AI) or P-Impedance (Ip), is determined by minimizing an objective (cost) function that contains multiple terms called misfit functions. The final merged model was created by merging the solid model and the SSI. In this process, the high vertical resolution of the well data and the high spatial resolution of the 3D Seismic data were combined to give a seismically constrained high-resolution impedance volume which gives a better estimation of inter-well reservoir properties. This was initially tested on several test lines before generating the final volume covering the entire area of interest. The inverse model was built using data from K-10 well while K-01 and K-02 wells served as blind wells, that is, wells that were not used in the inversion building process.

Porosity Modelling

The first step was to compute porosity log at the three wells. Reservoir porosity was determined from the density logs using the density equation (Equ. 1.0) (Wyllie et al., 1958). An average matrix density of 2.65g/cc for quartz was used. This was based on the grain density measurement from routine core analysis of the cored wells. In addition, fluid density (ρfl) of 1.01g/cc was used as the density of mud filtrate in the flushed zone at near well bore region. Following correction for gas effects, a reasonable estimate porosity at well locations for the reservoirs encountered was made.

$$\phi = (\rho_{ma} - \rho_b)/(\rho_{ma} - \rho_{fl}) \quad (1.0)$$

where

ρ_{ma} = matrix density

ρ_b = bulk density

ρ_{fl} = apparent fluid density

Secondly, Porosity-AI relationship was derived in TechLog software through regression analysis of the porosity against the impedance. We start with a presentation of the crossplot of P-impedance vs Porosity for K-01, K-10, and K-02 (see Figure 5).

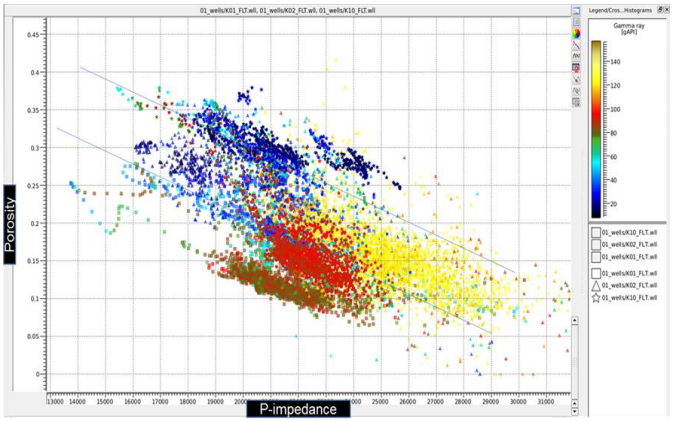

Figure 5: Cross plot of P-Impedance versus Porosity for the 3 Wells colored by Gamma ray (wide data point scatter indicates need to discretize analysis of overburden and reservoir sections)

The AI-Porosity cross plot clearly reveals different AI-Porosity data cloud and by implication, different trends between overburden and reservoir sections (Figure 6 middle). When the reservoir section is isolated, no clear trend could be found over entire reservoir section (Figure 6 right). This also revealed the need to discretize the reservoir sections in deriving a plausible trend. These present significant challenges in the 3D porosity volume estimation from a Seismically-Constrained Reservoir modelling in Kakawa Field. Additional log data were integrated to understand how to discretize the reservoir section. The sonic (compressional and shear) and density logs demonstrated a trend break at depth around 9500 ftss, or between D and E reservoir units. Remember that the objective reservoir for this study is the E1000. As a result, reservoir section was divided into two intervals. The upper interval shows normal trend and lower interval seems much compacted. See Figure 7.

AI-Porosity functions were built for each interval, using multi-linear regression, incorporating the compaction trend by burial depth.

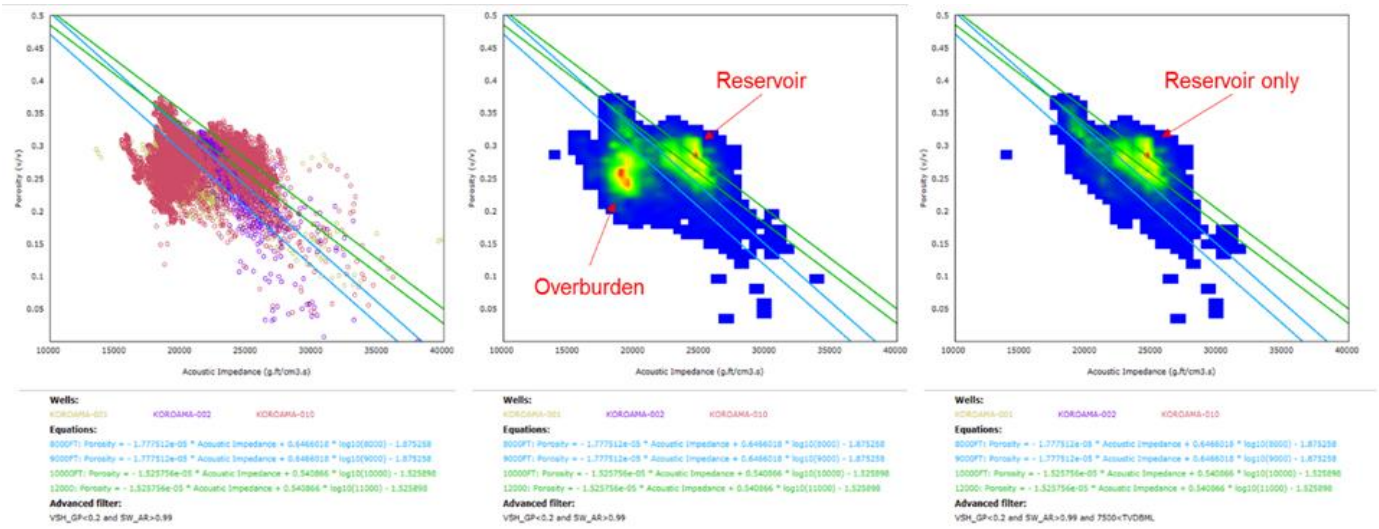

Figure 6: Porosity-AI relationship in the overburden & reservoir: Cross plot of P-Impedance versus Porosity for Wells K-01, K-02 and K-10 showing different cloud for overburden and reservoir sections

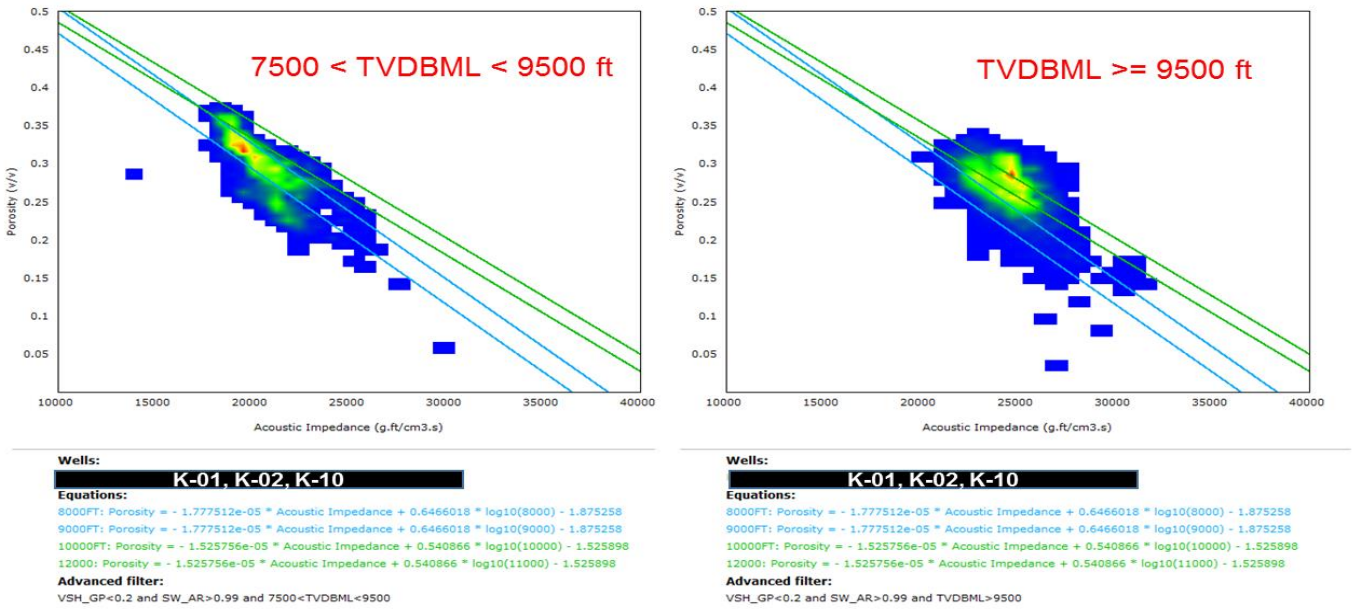

Figure 7: Porosity-AI relationship in the reservoir: Cross plot of P-Impedance versus Porosity for the 3 Wells showing different trends for shallow and deep reservoir sections

The following Porosity-AI relationship was derived for the deeper reservoir section including E1000

Porosity = - 1.525756E-05 * AI + 0.540866 * log10(DEPTH) - 1.525898 (2)

RESULTS AND DISCUSSION

The inverted volumes for the band-passed (relative) and full band (absolute) acoustic impedances were examined in track and bin directions and arbitrary traverses intersecting the key wells used in this study. The inverse model was built using data from K-10 well while K-01 and K-02 wells served as blind wells, that is, wells that were not used in the inversion building process.

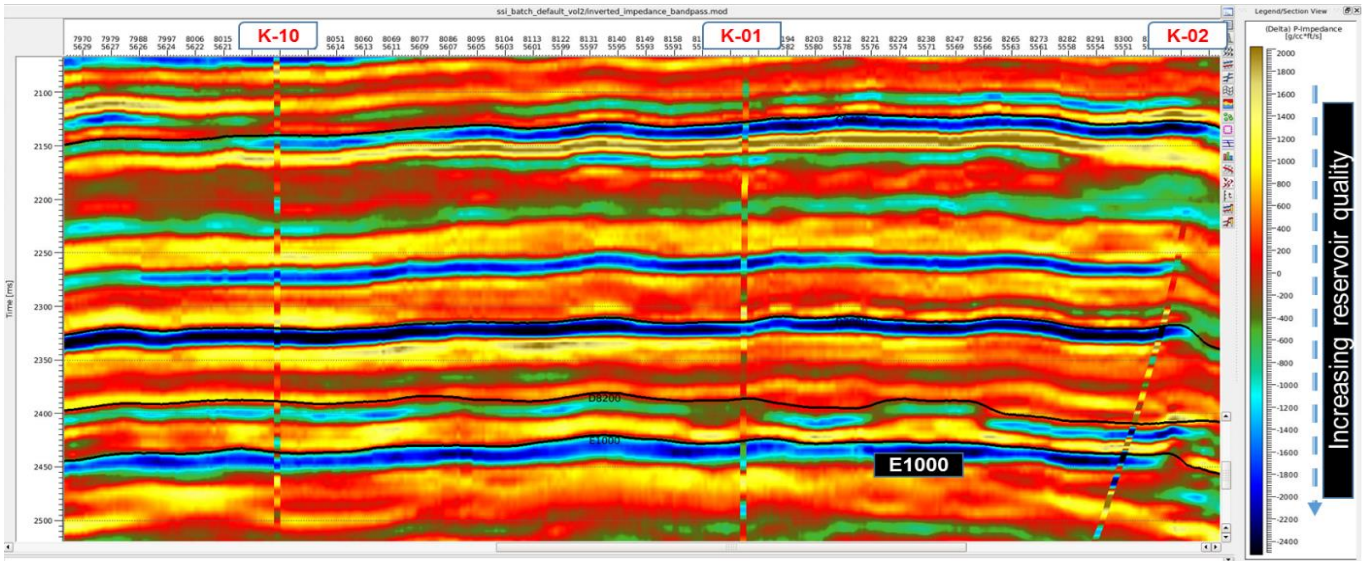

Figure 8: Band-passed P-impedance section intersecting well trajectories and superimposed at well locations by band-passed frequency filtered P-impedance well logs

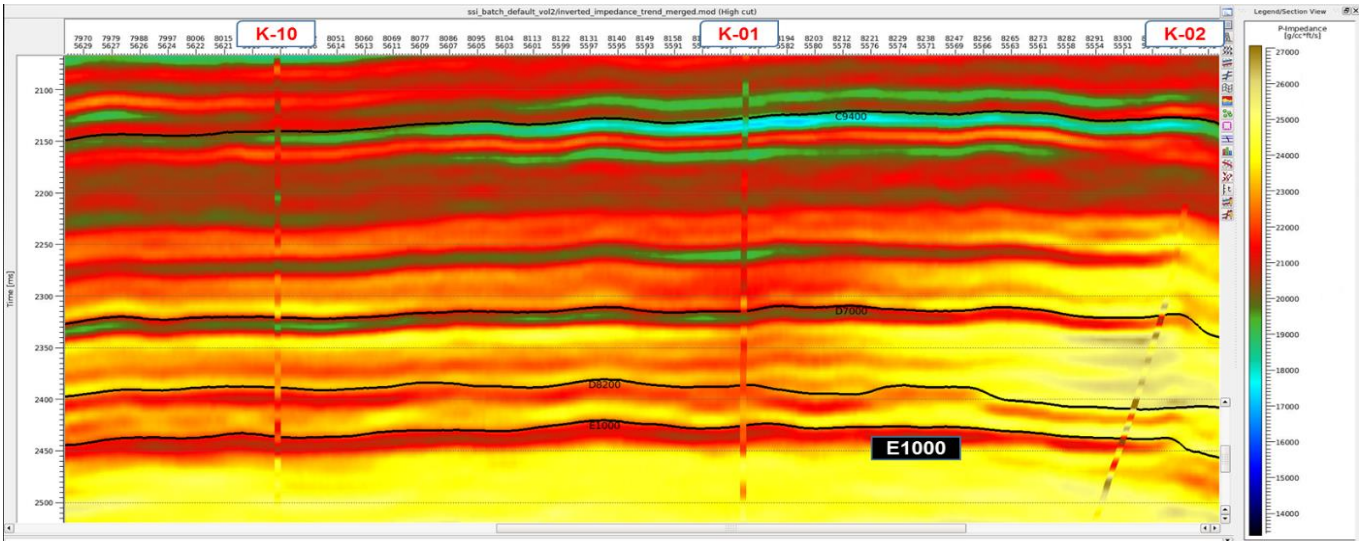

Figure 9: Absolute P-impedance section intersecting well trajectories at input and blind well locations

Figures 8 and 9 show section view panels of the derived impedance model in color density mode superimposed at well locations by wireline impedance log for both relative and absolute impedances. Generally, a good agreement exists between the model and log-based impedance across the E1000 reservoir. In addition, the seismic impedance results were checked using blind wells. In all cases results showed very good calibration at blind well locations.

The quality of the seismic inversion product was checked to ensure it is an adequate input into porosity volume estimation by various ways. The cross plot of the original well log P-Impedance with the P-Impedance extracted from the inverted volume along the well track was particularly interesting. Using the 3 wells for this calibration, notice the points in the cross plot form a tight distribution along the diagonal. However, some outliers or scatters were observed in the higher impedance value data points (see Figure 10 left). This is due to the poor quality of data from one of the wells. To improve results, this well was eliminated from the subsequent cross plot (Figure 10 right). In all cross plots, as characteristics of good quality inversion, we have a linear regression, with correlation greater than 91% and gradient of 1 (approx.).

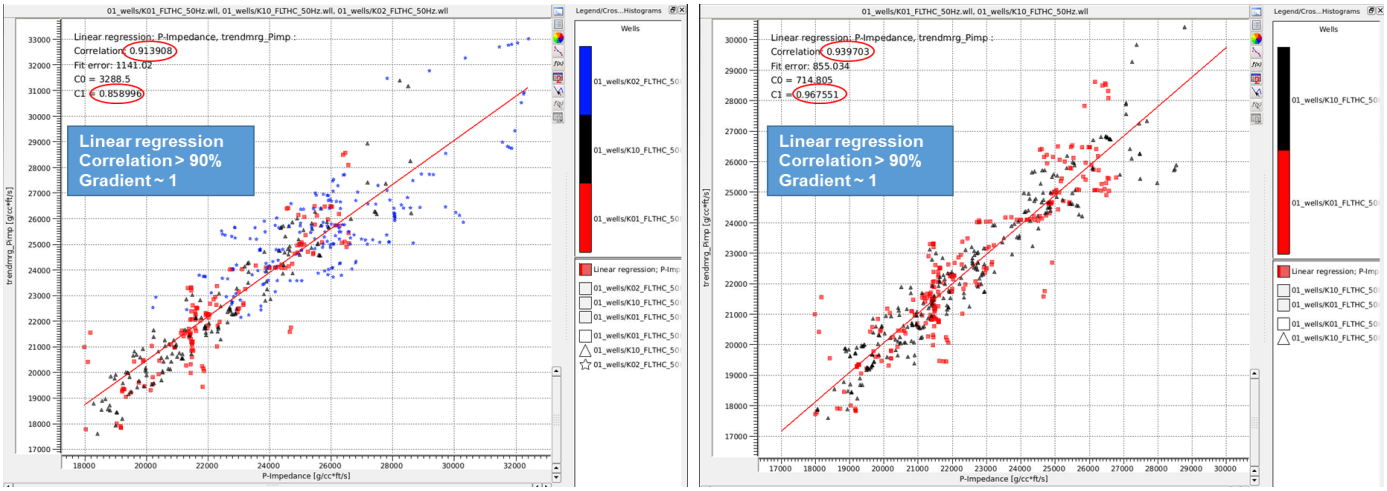

Figure 10: Left: crossplot with 3 wells showing a correlation of > 91%; Right: crossplot with 2 wells showing a correlation of > 93%

The next evaluation of result was carried out using the synthetic-to-seismic correlation map of E1000 horizon, generated during the inversion process. As shown in Figure 11, the values for this horizon are the cross-correlation between the seismic data and the synthetics generated from the sparse spike inversion result. This shows by how much the error norm was minimized. Put this differently, this refers to the degree of similarity achieved between the forward model (synthetic) and the actual measured seismic data. A correlation of 1 or 100% percent implies there is no

difference between the two datasets. For this study, a minimum correlation of 95% was achieved.

Another assessment of result captured in Figures 12 is the comparison of the measured well logs with extracted logs from the inversion in limited and full bandwidth respectively. A detailed comparison of the well log P-impedance to the inversion results was done by creating a pseudo log. We look at pseudo logs in full band and bandlimited displays. The bandlimited results do not have any of the low frequency model included. What is expected for good quality seismic inversion is for those pseudo logs to track each other. Overlaying the logs, in wiggle form, on the inversion result or extracting a pseudo log and comparing it to the real impedance log gives you a way to see which zones are not showing a good match between the inversion result and the actual log data. While there are areas of slight mismatch, notice very good match both in qualitative and quantitative terms.

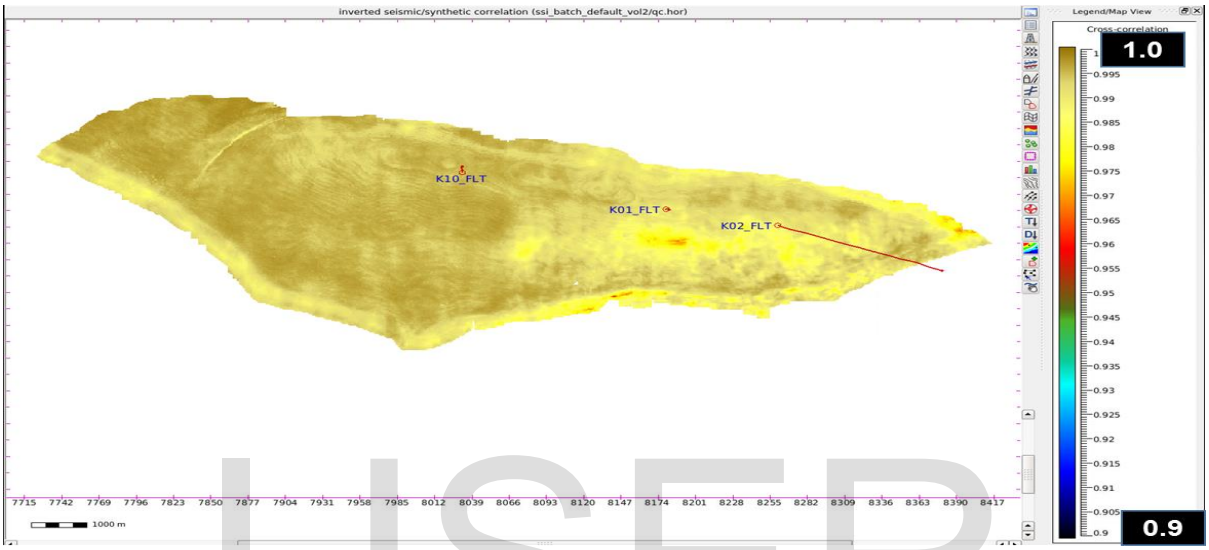

Figure 11: Seismic-Synthetic cross correlation map display of QC horizon of E1000 showing very high correlation

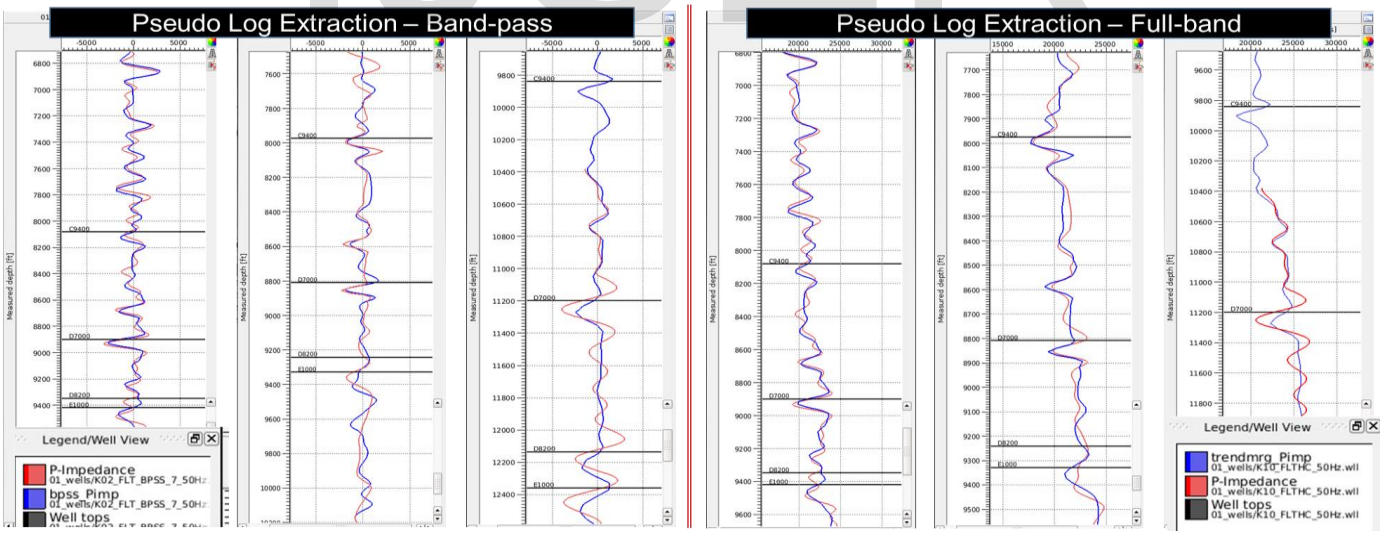

Figure 12: Pseudo log comparison of acoustic impedance from Well and Inverse model for both band-pass (left) and full-band (right)

The validity of inversion derived acoustic impedance as it relates to reservoir property (porosity) is the single most important source of uncertainty. Choice of seismic wavelet, quality of well-to-seismic tie and quality of the input RFC data – all have influence on the resulting impedance product. Careful log conditioning and rock physics analysis are important tools in reservoir characterization. In this case, they were helpful in arriving at a reasonable AI-porosity trend used in converting the acoustic impedance volume to a porosity volume

Estimated Porosity Volume

The estimated porosity cube was analyzed for agreement with measured porosities at well locations. Figure 13 (left) shows porosity section through different reservoirs. Figure 13 (Right) shows inline section of porosity volume at

intersection with well K-10. Result shows both qualitative and quantitative match with measured porosity at E1000. Figure 14 is a zoomed section of porosity volume at E1000 reservoir showing great match at wells K-10 and K-02. However, we also observe a mismatch at well K-01 due to the poor quality of input petrophysical log. In Figure 15 we look at porosity map of E1000 reservoir showing key wells

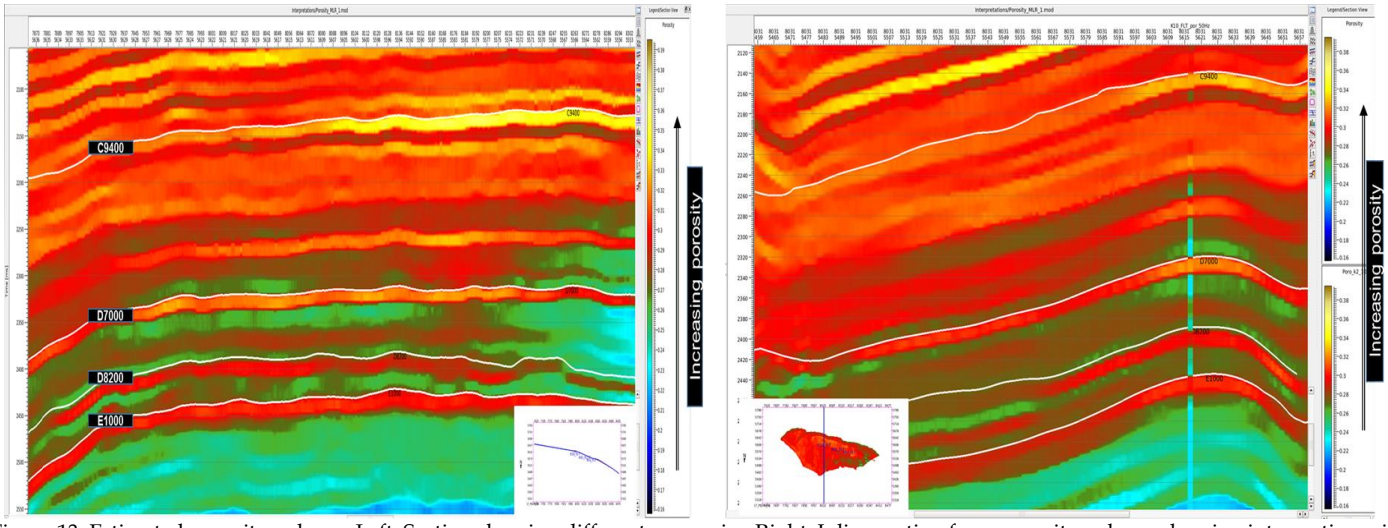

Figure 13: Estimated porosity volume. Left: Section showing different reservoirs; Right: Inline section from porosity volume showing intersection with well K-10. Result shows both qualitative and quantitative match with measured porosity at E1000

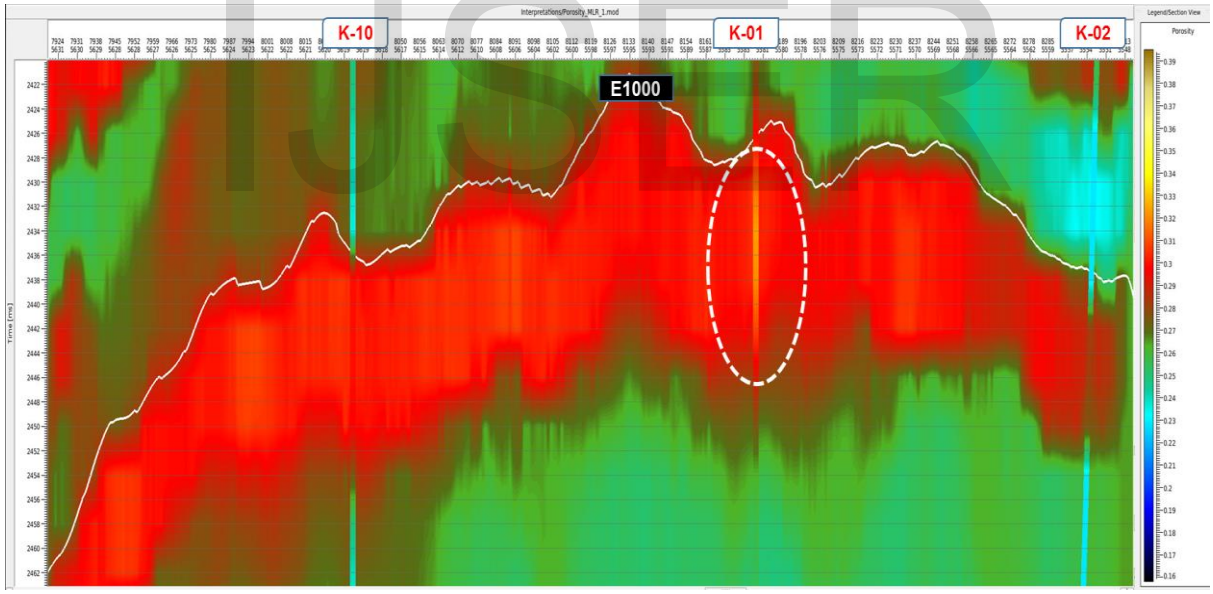

Figure 14: Zoomed section of porosity volume at E1000 reservoir showing great match at wells K-10 and K-02. Observe the mismatch at well K-01 due to the poor quality of input petrophysical logs

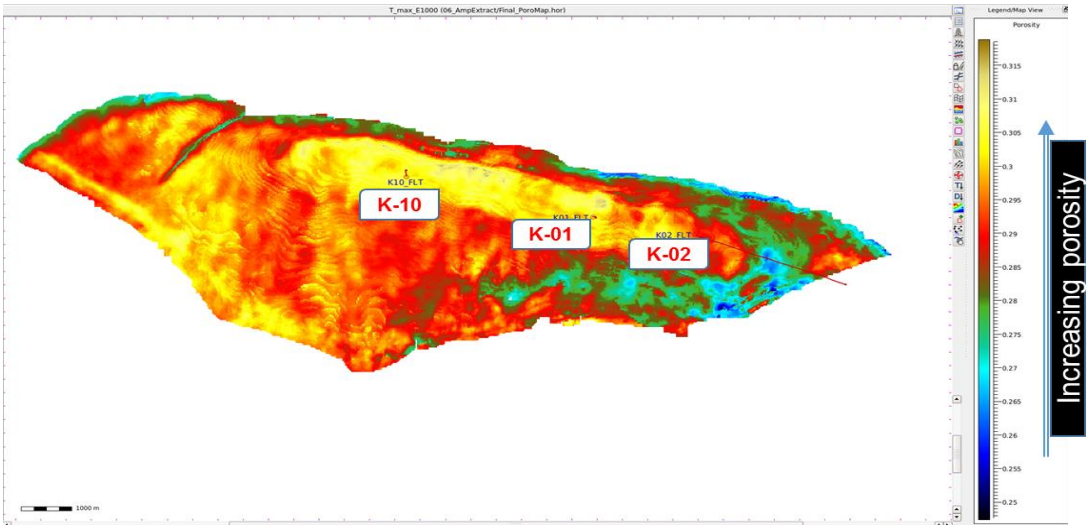

Figure 15: Porosity map of E1000 reservoir showing key wells

Maps and volumes generated from seismic data could suffer from vertical resolution issues which are in tens of meters. Thus, seismically derived porosity maps have the effect of averaging vertically, reducing variations in porosity that may be significant at reservoir characterization scale. For reservoir simulation work where, finer vertical details are required, it is perhaps better handled through simulation or stochastic techniques based upon residual distribution. Despite vertical resolution limitations, seismic inversion provides powerful information for predicting lateral variations in reservoir quality, not accessible through well data.

Well	Log Derived Porosity	Modeled Porosity
K-10	0.301	0.299
K-01	0.238	0.278
K-02	0.284	0.281

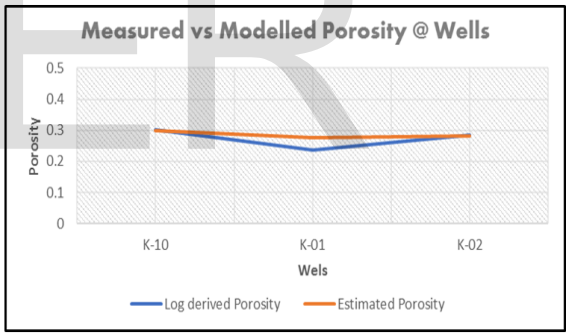

Figure 16: Porosity comparison: Measured vs modeled (numerically – left, graphically – right).

Reservoir development was assessed using maps and sections of relative impedance volume. Inversion reveals the objective sand (E1000) is well developed with variable thickness and quality. Away from the wells along the flank of the structure the quality of the reservoir sands appears to decay, possibly more heterolytic. This is illustrated in acoustic impedance section view captured in Figure 17. E1000 reservoir sand shows variable thickness and quality, suggesting channel deposits in a shoreface environment. For channel dominated deposits like the E1000 sands, care must be taken not to over rely on regional analogues to make general assumptions of good lateral sand development. It is critical to build specific multi-scenario models, capturing variations inherent in channel dominated setting. Appraising the full structure before full development remains key, as the extra calibration points helps in better definition of reservoir in terms or structure and quality. To identify appraisal possibilities, body checking should be carried out to highlight continuous porosity bodies. Porosity cubes of various porosity ranges should be created to analyse the continuous porosity bodies in the field and bounding prospects. These bodies should guide the location of well trajectories during development of field. What is clear though is that there is better sand quality at the crest of the structure. Appraisal wells K-10, K-10 and K-02 are seen not to target the best sand quality, hence providing scope for development.

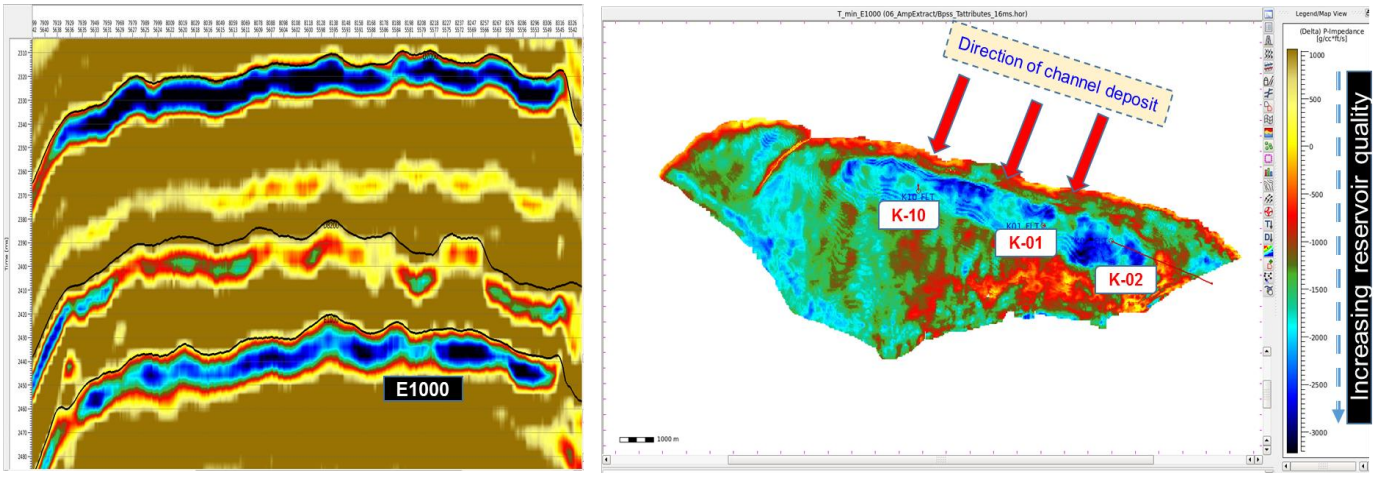

Figure 17: Understanding Sand development of E1000 reservoir. Left: Acoustic impedance volume showing section through E1000. Right: E1000 sand development map and direction of channel deposit

CONCLUSION

Rock physics modeling allowed us to characterize the E1000 reservoir sand at Kakawa Field through very good estimation of porosities from seismic data using post-stack inversion technique. Robust feasibility analysis assisted with better understanding and assessment of the quality and suitability of the current 3D seismic and well data for reservoir characterization and provided a framework for interpreting the resultant acoustic impedance volume.

The use of borrowed check shot (velocity function) and deviation of the well affected the well-to-seismic ties and impacted on the quality of extracted wavelet for seismic inversion. This challenge was mitigated using average wavelet, with the risk of reduced accuracy on derived acoustic impedance in the case of a spatially varying wavelet.

A strong relation between AI and measured Porosity was found, which varies with depth due to compaction effects. Based on this observation, multi-level AI-porosity transform was used to compute reasonable porosity volume over the reservoir of interest. The estimated porosity showed a good match with the porosity log at wells K-02 and K-10. Porosity estimates at K-01 well showed less accurate match due to the quality of the input petrophysical logs.

The seismic-inverted impedances and porosity estimated from seismic matched the well impedances (> 90% correlation) and measured porosities; the inversion process was validated through blind well testing.

Derived acoustic impedance volumes provided basis for assessing lateral variability and extent of the reservoir and aided assurance/validation of seismic interpretation.

Generated seismically constrained porosity volume should serve as a solid input into detailed static and dynamic modelling and well planning.

REFERENCES

Aki, K., and P. G. Richards, 1980, Quantitative seismology: Theory and methods: San Francisco, W.H. Freeman and Company, v. 1, 557 p.

Angeleri, G.P., and Carpi, R., 1982, Porosity prediction from seismic data: Geophys. Prosp., v.30, p.580- 607.

Buland, A., and Omre, H., 2003b, Bayesian wavelet estimation from well data and seismic; Geophysics, 68, 2000 2009.

Hampson, D., and Galbraith, M., 1981, Wavelet extraction by sonic-log correlation: Journal of the CSEG, v. 17, p. 24- 42.

Hampson, D., and Russell, B., 1985, Maximum-Likelihood seismic inversion (abstract no. SP-16)- National Canadian CSEG meeting, Calgary, Alberta.

Horfall, O. I., Uko, E. D., Tamunoberetoan-ari, I., and Omubo-Pepple, V. B. (2017). Rock-Physics and Seismic-Inversion Based Reservoir Characterization of AKOS FIELD, Coastal Swamp Depobelt, Niger Delta, Nigeria. IOSR Journal of Applied Geology and Geophysics (IOSR-JAGG) 5(4), 59-67.

Tamunobereton-ari, Iyeneomie. (2014). POROSITY MODELING OF THE SOUTH-EAST NIGER DELTA BASIN, NIGERIA. International Journal of Geology, Earth and Environmental Sciences. 4. 49-60.